



**STScI** | SPACE TELESCOPE  
SCIENCE INSTITUTE

Instrument Science Report ACS 2017-01

# Sink Pixels in ACS/WFC

---

J. E. Ryon, N. A. Grogin

February 24, 2017

---

## ABSTRACT

*We investigate the properties of sink pixels in the Advanced Camera for Surveys (ACS) Wide Field Channel (WFC) detector. These pixels likely contain extra charge traps and therefore appear anomalously low in images with relatively high backgrounds. We identify sink pixels in the average short (0.5-second) dark image from each monthly anneal cycle, which, since January 2015, have been post-flashed to a background of about  $60 e^-$ . Sink pixels can affect the pixels immediately above and below them in the same column, resulting in high downstream pixels and low trails of upstream pixels. We determine typical trail lengths for sink pixels of different depths at various background levels. We create a reference image, one for each anneal cycle since January 2015, that will be used to flag sink pixels and the adjacent affected pixels in science images.*

---

## 1 Introduction

First studied in the Wide Field Camera 3 UVIS channel (WFC3/UVIS) by Anderson & Baggett (2014a,b), sink pixels (SPs) are certain pixels in the detector that are consistently low compared to the background, likely due to an excess of charge traps located in those pixels. In WFC3/UVIS, SPs make up about 0.25% of the total number of pixels in the detector. However, depending on the depth of the SP and the background level of the image, several adjacent pixels may also be impacted. A total of  $\sim 1\%$  of the pixels in WFC3/UVIS were found to be affected by nearby SPs.

ACS/WFC began flashing its darks in January 2015 (Ogaz et al., 2015). About fifty long (1000.5-second) and short (0.5-second) darks are taken during each anneal cycle, and both

are post-flashed to the same average background level of about  $60 e^-$ . To produce the dark reference file for a given anneal cycle, the average short dark is subtracted from the average long dark to remove the post-flash electrons and 0.5 seconds of dark current. However, the post-flashed short darks also reveal a population of consistently low-value pixels that exhibit many of the same characteristics as the SPs studied by Anderson & Baggett (2014a,b) in WFC3/UVIS.

SPs often appear as individual pixels with anomalously low values, but can also give rise to a trail of low pixel values extending in the opposite direction to the readout direction for each chip. If the background level of the image is high, then most or perhaps all of the traps in a given SP will be filled, preventing these trapped electrons from being transferred to the readout register with the rest of the electrons in the SP. The SP will appear as a delta-function-like dip in the pixel values along a column. However, if the background is low, then the SP will trap a number of electrons from each of the upstream pixels as the image is read out, giving rise to low trails extending upstream of the SP. Charge transfer efficiency (CTE) effects may also contribute to smearing out the shape of a delta-function-like SP as it is read out.

In this report, we describe the properties of the SPs in ACS/WFC and a method for flagging them in images from January 2015 onward. We also identify upstream and downstream pixels that have been affected by the presence of adjacent SPs. We produce new reference images, one per anneal cycle, to be implemented in the next iteration of CALACS. The reference images will be used to flag SPs and the pixels they affect in the data quality (DQ) extensions of ACS images.

## 2 Observations

We select SPs from non-CTE-corrected short darks taken as part of the ACS CCD Daily Monitor calibration program (PI Golimowski) from January 2015 through the present<sup>1</sup>. We also use the non-CTE-corrected long darks to study the dark current behavior of the SPs. The short and long darks have exposure times of 0.5 and 1000.5 seconds respectively, and are post-flashed to a background level of about  $60 e^-$  (FLASHDUR = 4.6 seconds). The darks are processed through **acsccd** in CALACS and average-combined with positive-outlier clipping to reject cosmic rays. This results in a single short dark and a single long base dark, both bias-corrected and trimmed of overscan regions, for each anneal cycle<sup>2</sup>.

We also use 25-second darks taken as part of CAL-14865 (PI Anderson) to identify the typical length of trails for given SP depths and background levels. This program was allocated 12 internal orbits and was carried out on Nov 7 and 8, 2016, resulting in 28 darks post-flashed for different flash durations. This led to a well-sampled range of post-flash background levels between 0 and  $250 e^-$ . These darks were also processed through **acsccd** in CALACS, but since only a single dark was taken at each flash duration, they were not

---

<sup>1</sup>From programs CAL-13952, 13953, 13954, 14395, 14396, 14397. We do not identify SPs prior to January 2015 because the added post-flash background in the short darks is what allows us to detect SPs, and post-flashed darks are only available after January 2015.

<sup>2</sup>The base dark is then combined with day darks, and the short dark is subtracted to remove the flash electrons. This results in the final superdark reference files, of which there are 12 per anneal cycle.

combined.

We also use un-flashed long darks from CAL-14447 (PI Grogin) to find the average SP profile at low background (Section 4). These darks were processed through `acsccd` in CALACS and average-combined on a bi-weekly basis, resulting in two long darks. We use the second bi-week average dark from this program in Section 4.

### 3 Selecting Sink Pixels

To select SPs present in the detector for a given anneal cycle, we first subtract the flash electrons from the average short dark. We multiply the appropriate flash reference file for the anneal cycle by the flash duration and smooth it with a  $7 \times 7$  pixel boxcar kernel<sup>3</sup>. We smooth the flash reference image to remove artifacts associated with saturated areas near hot pixels, which would introduce very negative pixel values into the short dark. This procedure, however, does not remove detector artifacts present in the flat-field that also introduce negative values into the short dark (possibly the “freckles” noted in Bohlin et al., 2001). We mask the largest of these artifacts before SP selection.

Next, we consider the distribution of pixel values in the flash-subtracted short dark. Figure 1 shows such a distribution for the average short dark from the 2016-09-25 (Sept. 25, 2016) anneal cycle. Two columns of very low pixel values in Amp A (located at  $x = 1457, 1458$ ) appeared as a significant bump at the negative end of the distribution. The pixel values of these two columns are very negative in all of the 2015 and 2016 average short darks, and were therefore masked so as not to identify them as SPs. We also mask five other columns, one in WFC1 ( $x = 2156$ ) and four in WFC2 ( $x = 350, 2500, 3128, 3164$ ), that were found to have significantly more negative pixels than a typical column. These masked columns do not appear in Figure 1.

Because there is very little dark current in a 0.5-second dark, the peak of the distribution in Figure 1 lies essentially at zero. Warm and hot pixels appear as a tail to the positive side of the peak. SPs are located in the tail to the negative side of the peak. A clear departure from typical Poisson behavior is seen as a linear trend in the distribution  $\lesssim -10 e^-$ .

We determine the location of the breakpoint between the Poisson and linear trends in the histogram by Markov Chain Monte Carlo (MCMC) sampling of a likelihood function. We assume the distribution of pixel values between  $-30$  and  $0 e^-$  is represented by the sum of an exponential function and a Gaussian, based on the shape of the semi-log histogram over this domain. The likelihood function we define is:

$$\mathcal{L} = \exp\left(-\frac{(x - \bar{x})^2}{2\sigma^2}\right) + \alpha \exp\left(-\frac{x}{x_0}\right), \quad (1)$$

where  $x$  is the pixel value,  $\bar{x}$  and  $\sigma$  are the mean and standard deviation of the Gaussian, respectively,  $\alpha$  is a scale factor between the two components, and  $x_0$  controls the scale of the exponential function. The exponential component contains SPs and the Gaussian represents normal pixels. Next, we redefine  $x_0$  in terms of the location of the breakpoint,  $x_b$ , which we

---

<sup>3</sup>We used `Box2DKernel` and `convolve` in `astropy.convolution` to define the kernel and smooth the flash reference file.

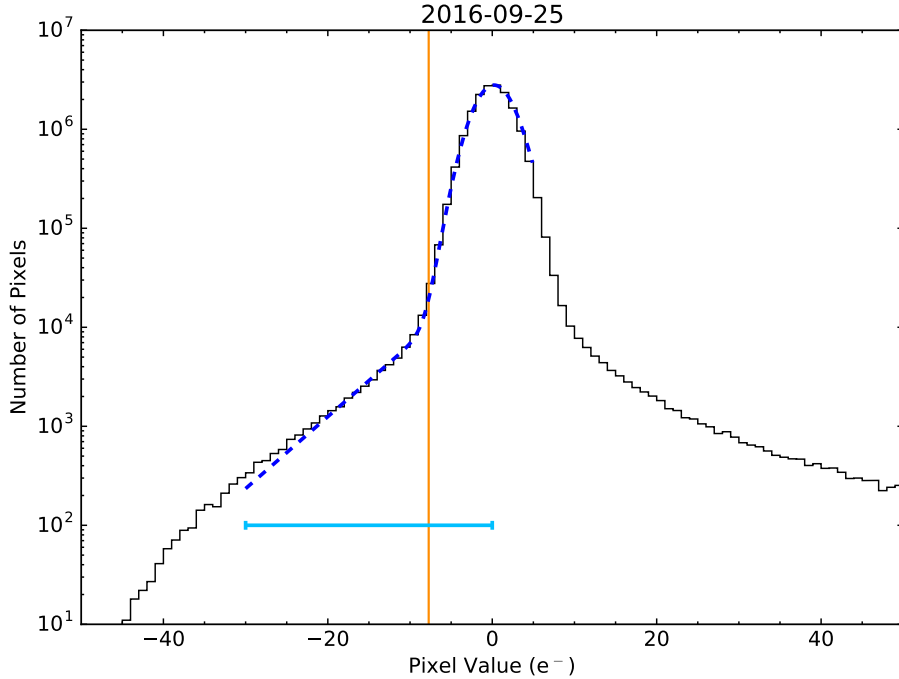


**Figure 1:** Pixel value histogram for the flash-subtracted short dark from the 2016-09-25 anneal cycle. The blue dashed line shows the likelihood function (Eq. 1) that best represents the pixel values in this anneal, as determined by MCMC sampling. The horizontal cyan line shows the range of pixel values over which the MCMC sampling was performed. The vertical orange line represents the location of the breakpoint,  $x_b$ , which is  $-7.7 e^-$  for this anneal.

define as the point where the likelihood of a pixel value falling in the Gaussian component is equal to that of a pixel value falling in the exponential component, or

$$x_0 = \frac{x_b}{\ln(\alpha) + \frac{(x_b - \bar{x})^2}{2\sigma^2}}. \quad (2)$$

This allows us to solve for  $x_b$  directly with the MCMC technique. We normalize Equation 1 over the range  $-30$  to  $0 e^-$ , and define priors to ensure that  $\sigma$  and  $\alpha$  are positive and  $x_b$  is negative. We calculate the log-likelihood and log-prior probabilities for computational ease, and sum them together. We use the MCMC sampler provided in the python package `emcee` to explore the likelihood space (Foreman-Mackey et al., 2013). We choose 100 walkers, each with different initial guesses for the four parameters of the likelihood. The initial guesses are determined by minimizing the negative log-likelihood with `optimize.minimize` within `scipy` and adding a small random offset to each parameter for each walker. We found that the walkers reached stable solutions after about 800 burn-in steps and 1200 chain steps. To determine the parameter values that best describe the pixel value distribution, we find the median of all of the walkers' chain steps for each parameter.

We use this MCMC technique on the flash-subtracted pixel values in the average short dark from each anneal cycle since January 2015. We find that the median parameters vary somewhat between anneal cycles. More specifically,  $\bar{x}$  ranges between  $\sim 0$  and  $0.8 e^-$ ,  $\sigma$

between 2.0 and 2.4  $e^-$ ,  $x_b$  between  $-7.7$  and  $-6.3 e^-$ , and  $\alpha$  between 0.009 and 0.013. Therefore, pixel values near the breakpoint,  $x_b$ , are  $\sim 3$  to  $3.5\text{-}\sigma$  outliers from the typical background level. We estimate the number of pixels present in the Gaussian component and in the exponential component, and find that between  $\sim 3\%$  and  $18\%$  of the pixel values below the breakpoint may be normal pixels lying on the far negative end of the Gaussian distribution.

We identify all pixels in the short dark with values more negative than  $x_b$ , represented by the vertical orange line in Figure 1, for that anneal cycle. We want to avoid selecting the low trailing pixels as SPs because only the pixel containing charge traps should be considered an SP. For each low pixel value, we throw out other low pixel values directly upstream so that only the pixel closest to the amplifier in a given trail is selected as an SP. We select SPs in this way for each anneal cycle beginning with January 2015, and find between 59,000 and 74,000 SPs ( $0.35\%$  and  $0.44\%$  of the detector, respectively) in the average short dark from each anneal. The variation in the number of SPs identified is mostly due to variation in the breakpoint between anneals. We find a new breakpoint value for each anneal cycle because the number of short darks obtained during that cycle may be slightly different than the other anneals, and therefore the noise in the average short dark will change. This affects the width of the Gaussian peak in the pixel value distribution, which changes where the transition between the exponential SP tail and the Gaussian component occurs.

In Figure 2, we show a  $100 \times 100$  pixel<sup>2</sup> region of the flash-subtracted short dark for the 2016-09-25 anneal cycle. Darker color pixels have lower values, such that the most negative are black. SPs selected according to the algorithm described above are circled in orange.

On the left in Figure 3, we plot the distribution of SP depths as determined from the flash-subtracted average short dark for the 2016-09-25 anneal. The majority have depths between  $-7$  and  $-40 e^-$ , though there are several deeper SPs as well. On the right in Figure 3, we plot the values of these same pixels taken from the average long dark from the same anneal cycle, which has had both the post-flash and a local background removed<sup>4</sup>. While the peak in the distribution is located at about  $-5 e^-$  and the majority of the pixel values are negative, there are many pixels with higher values, some quite positive. Therefore, it appears that SPs can have substantial levels of dark current, making them appear warm or hot in long exposures.

## 4 Impact on Adjacent Pixels

We further investigate the trails of low pixels extending upstream from SPs. We do this by grouping SPs of similar depths (e.g.,  $-20 \pm 5 e^-$ ) and finding the median values of the 20 pixels in the same column, above and below each SP. In Figure 4, we plot the profiles for SPs of different depth in each of three panels. The SPs included in this plot were selected from the flash-subtracted short darks for the 2015-10-22 anneal cycle, but were also required to be negative in the un-flashed, local-background-subtracted long dark from the same anneal. This ensures that the SPs that experience higher levels of dark current are not included in our median profiles, since these would tend to artificially flatten the profiles. We use this

---

<sup>4</sup>We made a local background image by smoothing over the flash-subtracted long dark image with a  $7 \times 7$  pixel boxcar kernel. We then subtract this local background image from the long dark.

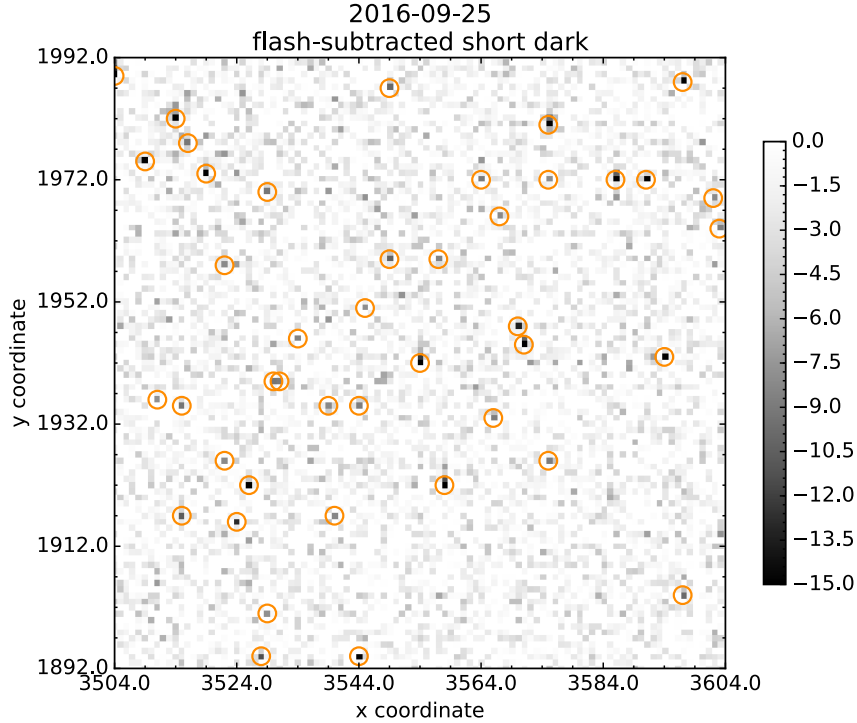


**Figure 2:** A  $100 \times 100$  pixel<sup>2</sup> region in the flash-subtracted short dark for the 2016-09-25 anneal cycle centered on a deep SP with a trail extending towards the top of the image. Trails are visible following some of the other SPs, but many appear to be individual pixels.

anneal cycle for this analysis because it is the only cycle during which both flashed and un-flashed darks were obtained.

In Figure 4, triangles with dashed lines correspond to SP profiles located in the half of the detector near the readout amplifier, and circles with solid lines are profiles located in the half far from the amplifier. The profiles for SPs on the WFC1 chip were flipped to match the orientation of the WFC2 profiles because the readout directions for the two chips are in the opposite sense. Profiles from the average short dark are plotted as blue curves, and profiles from the average, un-flashed long dark are plotted as orange curves. The post-flash background is higher towards the center of the detector, which is why the blue curves have a higher overall background level far from the amplifiers.

The SP profiles in Figure 4 exhibit many of the same characteristics as those presented by Anderson & Baggett (2014b) in their Figure 6. At high background levels, SPs of all depths appear similar to delta functions. The first pixel upstream from the SP (+1 on the x-axis of the plot) is also consistently lower than the background. SPs with more traps appear to pull down the values of the next few upstream pixels as well. In low background images, the SPs themselves do not appear as deep as in the high background images, but they affect several more upstream pixels. The shape of these profiles is likely due to the low-background images not having enough electrons to fill all of the traps, such that upstream pixels also lose electrons to the traps. It may also be the case that imperfect CTE effects fill in the leading edge of the SP profiles, making them less sharp.

Another interesting feature of the SP profiles is the excess of charge sometimes found

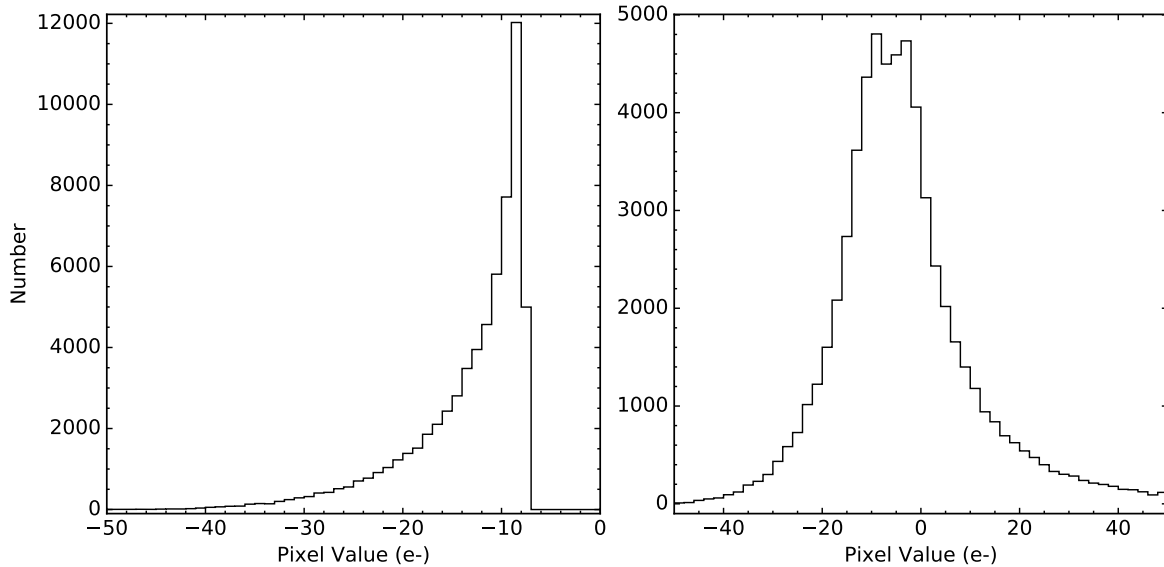


**Figure 3:** (left) Distribution of SP depths from the flash-subtracted short dark for the 2016-09-25 anneal. They range between  $-7.7$  and  $-40 e^-$ . The furthest right bin is partially filled because the breakpoint is  $-7.7 e^-$  for this anneal, and the bin goes from  $-7$  to  $-8$ . (right) Distribution of the SP values from the flash and local-background-subtracted long dark from the 2016-09-25 anneal. Some SP values are high relative to the local background in the long dark, suggesting that they have significant dark current.

in the downstream ( $-1$ ) pixel<sup>5</sup>. The excess appears to be more common for SPs near the amplifier than those far from the amplifier, but has about the same amplitude in both high- and low-background darks. On the left in Figure 5, we plot the flash-subtracted values of downstream pixels adjacent to a random selection of 20,000 SPs in the 2016-09-25 short dark. In the right panel, we plot the distribution of all of the downstream pixel values. Most of these pixels lie in a band near zero (i.e., they do not have a substantial excess relative to the background), but many others have large values. The upper envelope of points shows that the excess increases dramatically towards the bottom and top of the images (left and right in the plot), where the amplifiers are located. We identify those downstream pixels with values  $>5 e^-$  relative to the background for each anneal cycle in order to flag them. We select  $5 e^-$  as the lower limit, represented by the blue horizontal line in the figure, which corresponds to a  $2\text{-}\sigma$  deviation from the peak in the distribution of pixel values. About 28% of SPs in a given anneal are adjacent to a downstream pixel with a charge excess above  $5 e^-$ .

## 5 Determining Lengths of Sink Pixel Trails

In order to flag the trails of low pixels upstream of the SPs, we must determine the typical trail lengths for SPs of different depths at various background levels. To do this, we use the

<sup>5</sup>It is unknown why this excess charge appears in the downstream pixel, though Anderson & Baggett (2014a) suggest it may have to do with the way in which the detector is read out. Some of the electrons trapped in the SP may be “squeezed” out of the traps and deposited in the downstream pixel as voltage is applied to read out the detector.

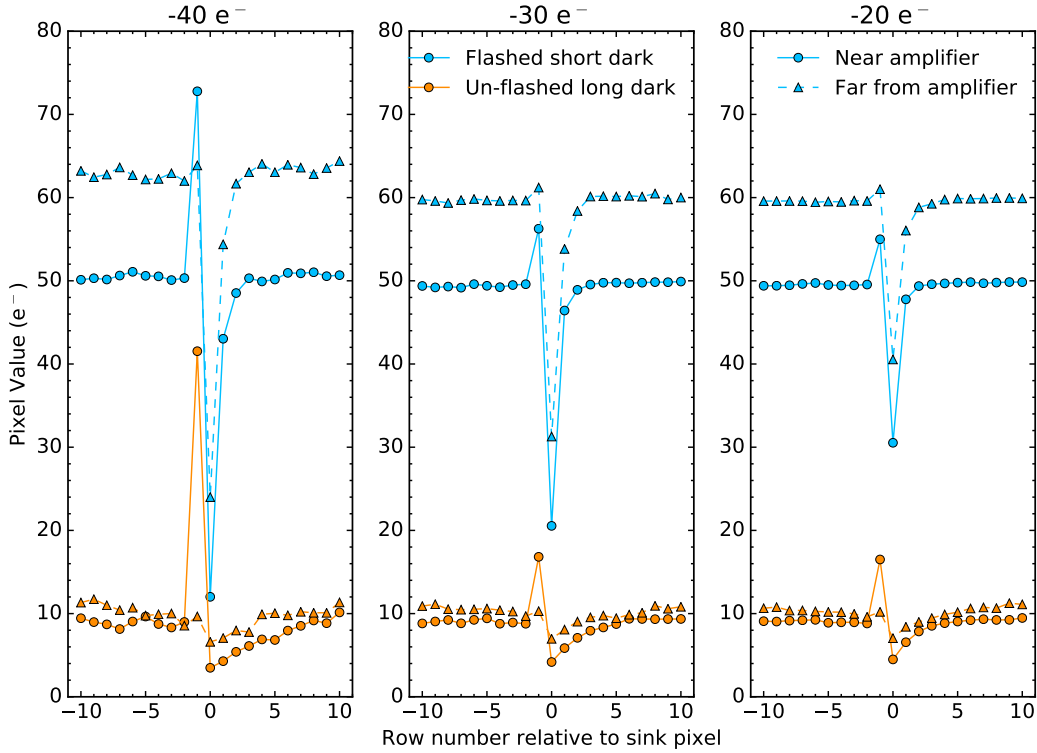


**Figure 4:** Median pixel values along the column for 20 pixels above and below SPs of different depths. From left to right, the panels show median profiles for SP depths of  $-40 \pm 5$ ,  $-30 \pm 5$ , and  $-20 \pm 5$   $e^-$ . The triangles with dashed lines represent SPs in the half of the detector near the amplifier, and the circles with solid lines represent SPs in the half far from the amplifier. The blue curves are from the average short dark and the orange curves are from the un-flashed long dark from the 2015-10-22 anneal cycle.

25-second darks taken as part of CAL-14865, each of which was post-flashed to a different background level. We identify the  $\sim 26,500$  SPs that are present in all of the anneals since January 2015 because they will likely appear in the 25-second darks as well.

We do not subtract the flash from the 25-second darks. For each dark, we first tabulate the value of each SP, the value of each of the 15 pixels upstream from each SP, and a local background value (median of  $7 \times 7$  pixel square around the SP). We then separate these data by the average SP depth across the 2015 and 2016 anneal cycles. This results in four bins of SP depth:  $-10 \pm 5$   $e^-$ ,  $-20 \pm 5$   $e^-$ ,  $-30 \pm 5$   $e^-$ , and  $< -35$   $e^-$ .

We make two sets of plots with these data. The first set, an example of which is shown in Figure 6, contains profiles similar to those presented in Figure 4. To make these profiles, we calculate the sigma-clipped average of each trailing pixel for a given SP depth ( $-20 \pm 5$   $e^-$  in the case of Figure 6) for each 25-second dark. The background level is represented by a dashed orange line, which is a sigma-clipped average of the local background values around the appropriate SPs. We create a plot like this for each bin of SP depths.

The second set of plots shows the local-background-subtracted value of each pixel in the trail upstream of SPs as a function of background level. For example, in Figure 7, we show the sigma-clipped average values of the second pixel upstream from the SP as measured

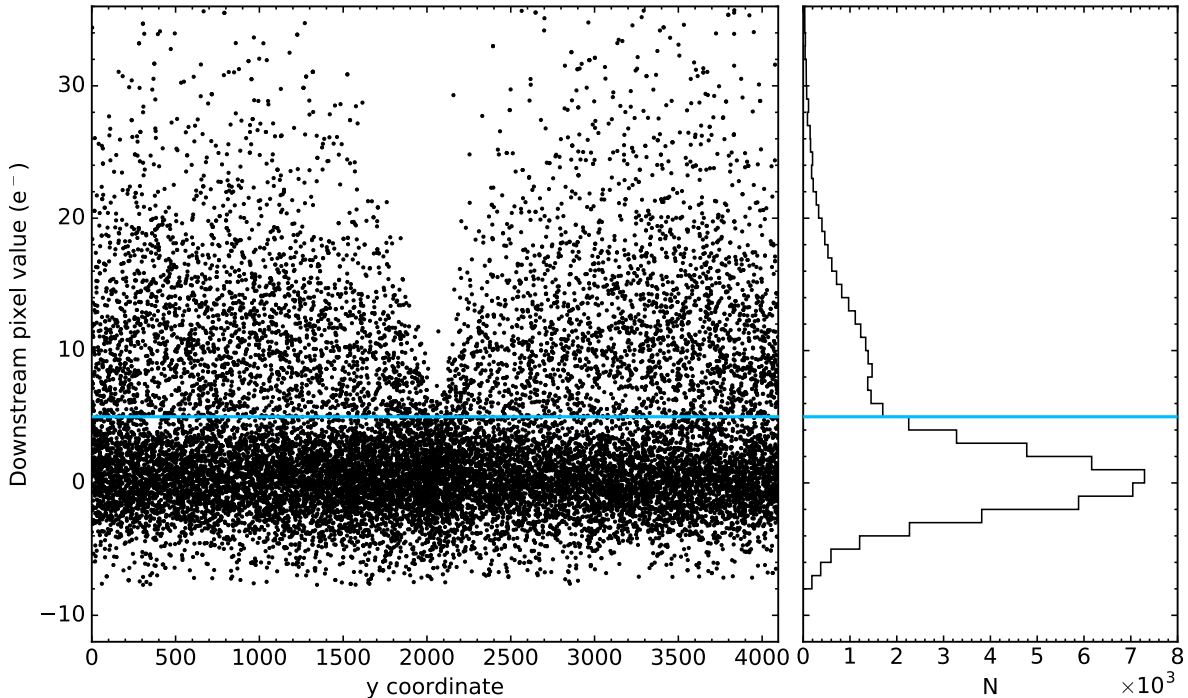


**Figure 5:** (left) Flash-subtracted values of pixels immediately downstream ( $-1$  pixel along the column) of 20,000 randomly-selected SPs identified in the 2016-09-25 average short dark as a function of row coordinate. (right) Distribution of values of all of the downstream pixels from this anneal. Downstream pixels that lie above the blue line ( $5 e^-$ ) have significant excess charge about  $2\text{-}\sigma$  above the background.

from the 25-second darks. Each of the four panels represents the four bins in SP depth. The location on the x-axis at which the points cross zero (the dashed black line) is an estimate of the background level required for that number pixel to no longer be influenced by the SP. We make a plot like this for each of 15 pixels upstream of the SP location.

By inspecting these two sets of plots, we estimate the background level at which each subsequent pixel in the trail appears to recover from the effects of the SP. From this, we build a preliminary reference table specifying (1) the upper and lower limits of the bin of SP depths, (2) the background level, and (3) the number of pixels that are affected by the SP at or below the specified background level. While this information is sufficient for identifying the appropriate number of trailing pixels for a given SP, it would be computationally expensive to determine the local background for each SP in every image. The non-flash-subtracted value of an SP encapsulates both the SP depth and the local background into a single number, and can therefore be used to determine when a given trailing pixel should be flagged. To determine the SP values that correspond to each SP depth and background level combination, we find the 25-second short dark with the nearest median background level. We identify the SPs in this image that correspond to the appropriate depth bin, calculate the sigma-clipped average value of these SPs, and add this value to the appropriate row in the table.

The portion of this reference table for SP depths  $-20 \pm 5 e^-$  is shown in Table 1, and should be read as follows. If the background level in an image is between  $50$  and  $150 e^-$ , for

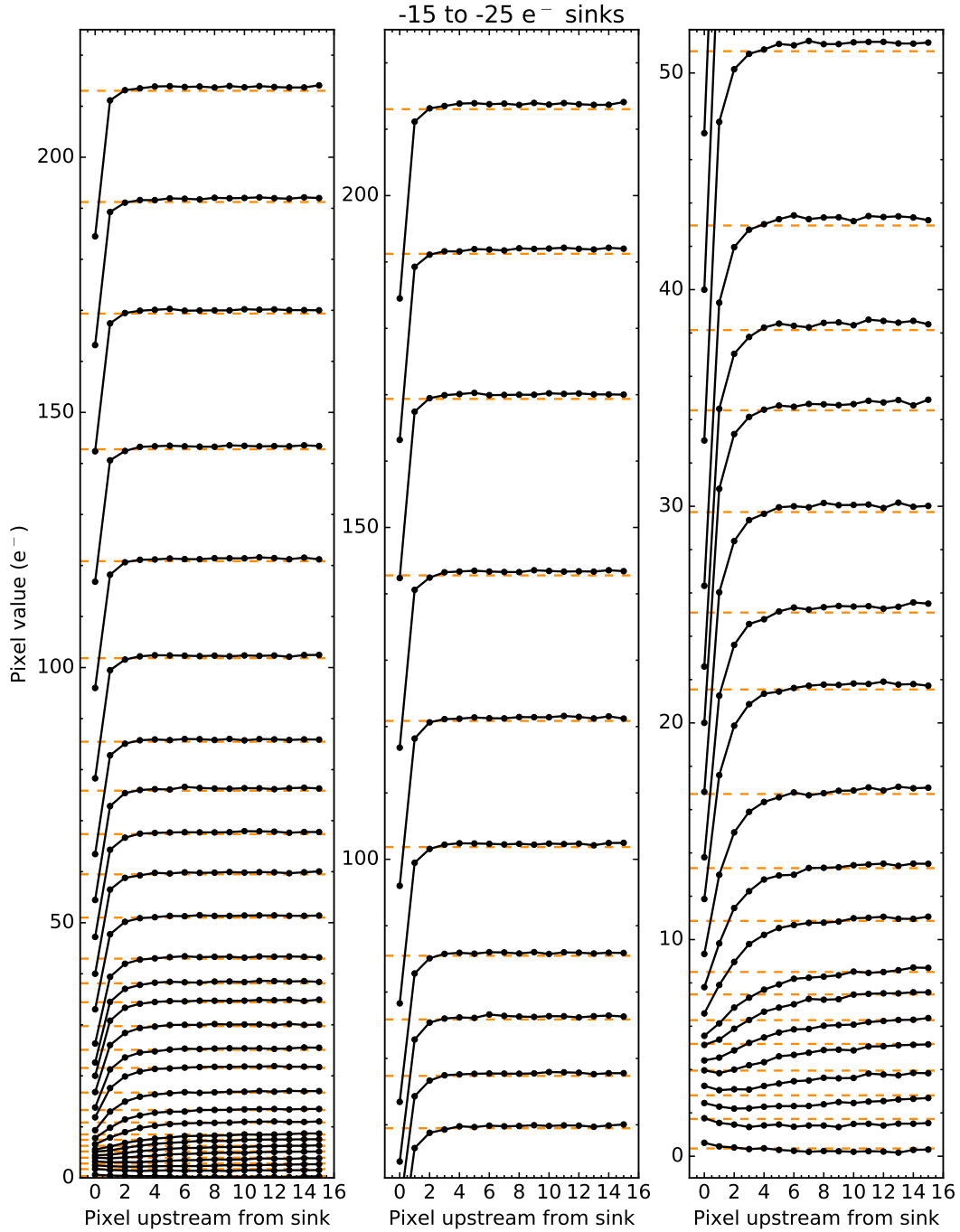


**Figure 6:** SP profiles from the 25-second darks with multiple flash levels. The SPs included in this plot have average depths of  $-20 \pm 5 e^-$  in the short darks from the anneal cycles between January 2015 and December 2016. The dashed orange lines are the sigma-clipped average local backgrounds around the SPs. The left panel shows all of the profiles, from backgrounds of about 0 to 220  $e^-$ . The middle panel provides a closer view of the profiles at high backgrounds, between about 52 and 220  $e^-$ , and the right panel shows only the profiles below 52  $e^-$  background.

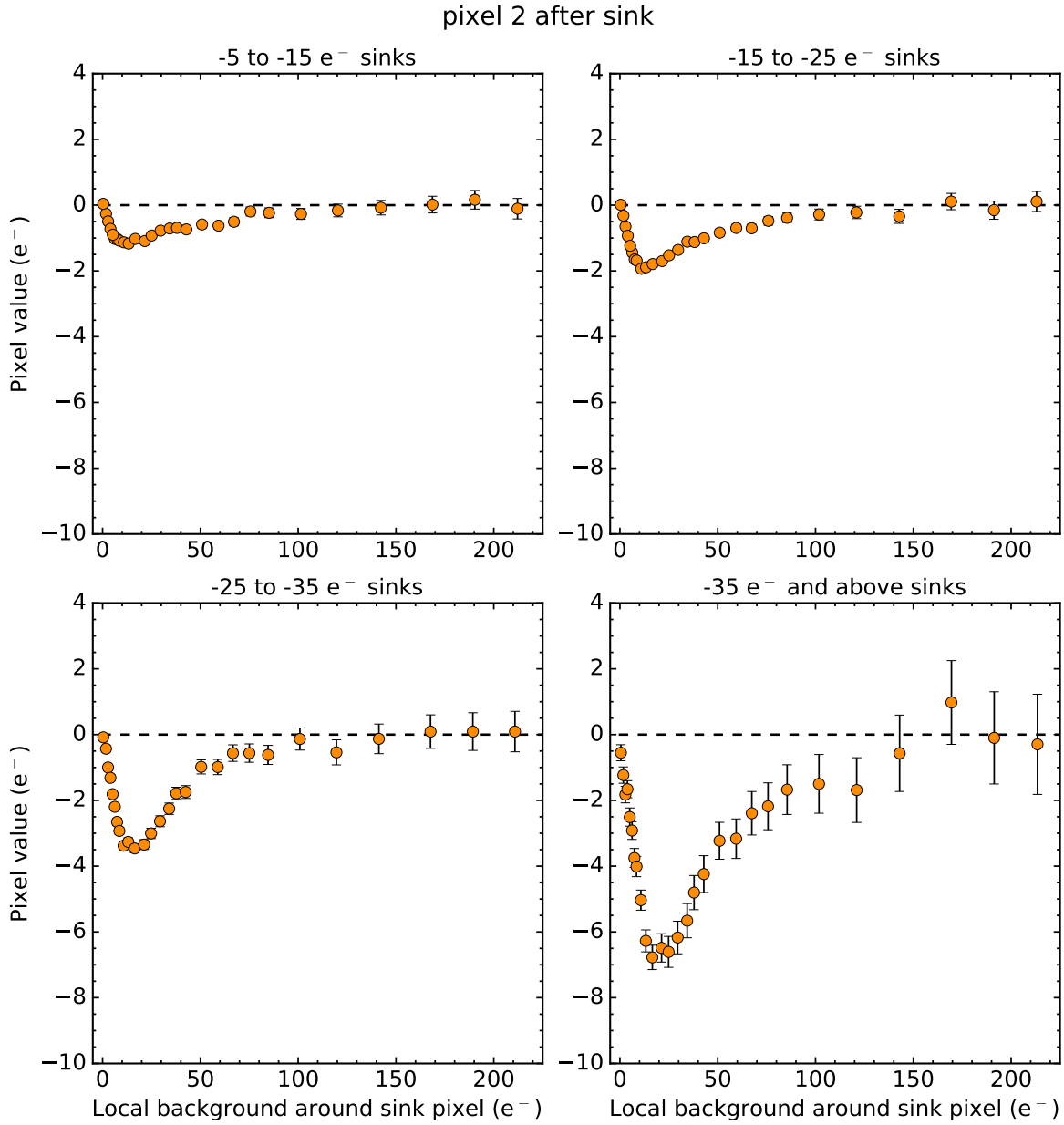


**Figure 7:** Sigma-clipped average value of the second pixel upstream from the SP (relative to the local background) as a function of background in the 25-second darks. Each panel represents a different SP depth bin. The dashed black line indicates where the pixel value is equal to the background level.

SP Depth Bin Limits ( $e^-$ )	Background ( $e^-$ )	Trail Length (pix)	SP Value ( $e^-$ )
-25 to -15	150	2	116.8
-25 to -15	50	3	33.0
-25 to -15	35	4	20.0
-25 to -15	20	5	11.9
-25 to -15	15	6	7.8
-25 to -15	10	7	6.6

**Table 1:** Reference table for determining the trail lengths for various SP depths and background levels. This is the portion of the table for SP depths of  $-20 \pm 5 e^-$ .

instance, then 2 pixels upstream from the SP should be flagged. In this case, the value of an SP of depth  $-20 \pm 5 e^-$  in the image (non-flash-subtracted) would be between 33.0 and 116.8  $e^-$ . We can therefore simply look at the actual value of an SP to determine how many pixels upstream from the SP to flag.

## 6 Creating and Applying the Reference Image

We follow the lead of Anderson & Baggett (2014b) in creating a reference FITS image containing all of the information necessary to properly flag SPs, trails, and high downstream pixels. We make one reference image for each anneal cycle from January 2015 onward. In the reference images, the location of each SP is assigned the depth of that SP as determined from the flash-subtracted short dark for the anneal cycle in question. If the downstream ( $-1$ ) pixel from the SP has a value  $>5 e^-$  in the flash-subtracted short dark, it is assigned a value of  $-1.0$ . The upstream ( $+1$ ) pixel from the SP is assigned the value 999.0 because it should be flagged for all but the highest of backgrounds. The next several upstream pixels (between  $+2$  and  $+7$  for SP depths of  $-20 \pm 5 e^-$ , for instance) are assigned the SP values listed in the reference table (Table 1). For SPs of depths  $-10 \pm 5 e^-$ , we assign values up to the  $+6$  pixel, for SPs of depths  $-30 \pm 5 e^-$ , we assign values up to the  $+9$  pixel, and for SPs of depths  $<-35 e^-$ , we assign values up to the  $+12$  pixel. Longer trails are therefore flagged for deeper sinks.

To apply the reference image to science exposures, we find the pixels with values less than  $-1.0$  in the reference image. These are the SPs, so we set the charge trap flag, 1024, for these pixels in the data quality (DQ) extension of the science image. If the downstream pixel from the SP is set to  $-1.0$ , then we activate the charge trap flag for that pixel as well. Next, we look at the first upstream pixel from the SP. If the value of the SP in the science image is less than the value of the upstream pixel in the reference image, then we activate the charge trap flag for that upstream pixel in the DQ extension of the science image. We continue along the column of the reference image in this fashion. Once the value of the pixels in the reference image return to zero, or the SP value in the science image is greater than that of the  $n$ -th upstream pixel in the reference image, we stop flagging for that SP. In this way, more pixels will be flagged in low background images than in high background images,

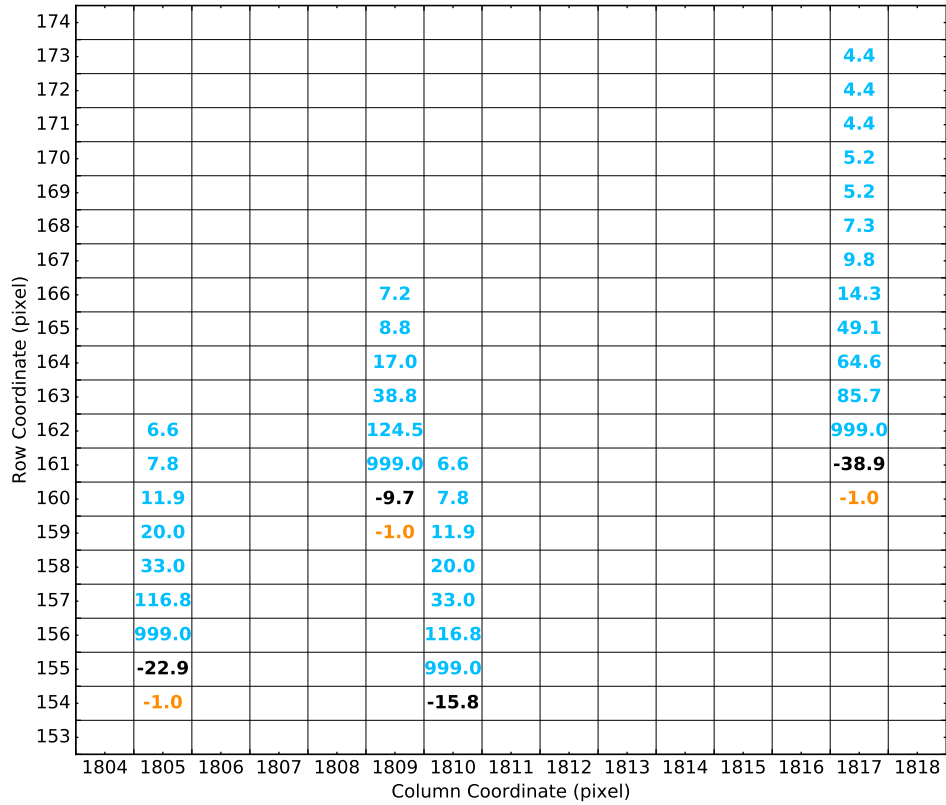


**Figure 8:** A small section of the reference image for the 2016-09-25 anneal cycle. Each square in the grid represents a pixel. Black numbers are the SP depths, of which there are two in the  $-20 \pm 5 e^-$  bin, one in the  $-10 \pm 5 e^-$  bin, and one in the  $< -35 e^-$  bin. Orange numbers are high downstream pixels and blue numbers are the upstream trails.

and more pixels will be flagged for deeper SPs than shallower SPs.

For the 2016-09-25 anneal cycle, the reference image contains 63,091 SPs, 17,910 high downstream pixels, and 398,575 upstream pixels, for a total of 479,576 pixels, or 2.9% of the detector. The actual number of pixels that will be flagged for a given science image depends on the background level of the image. Therefore, only for the lowest background science images will all 470,000+ pixels be flagged. The pixel values of a small section of the reference image for the 2016-09-25 anneal cycle is shown in Figure 8. The black numbers show the location and depth of the SPs, of which there are four in this plot. Three of the SPs have adjacent high downstream pixels, represented by the orange numbers, and the blue numbers show the assigned values of the upstream trailing pixels.

We tested the application of the reference image to two images, an individual short dark image from the 2016-09-25 anneal and an individual un-flashed long dark image from the 2015-10-22 anneal. These images have significantly different background levels, which is ideal for testing the number of upstream trailing pixels that are flagged under different conditions. For the short dark, which has a background level of  $\sim 60 e^-$ , we flagged about 231,000 pixels in total, or about 1.4% of the detector. For the un-flashed long dark, which has a background level of  $\sim 10 e^-$ , we flagged about 376,000 pixels, or 2.2% of the detector. Therefore, the reference image behaves as expected, flagging more upstream trail pixels in images with lower backgrounds.

## 7 Sink Pixel Creation and Persistence

By looking at the depths of SPs identified in one anneal over the other anneals, we can find SPs that have been created during this two-year baseline. The depths of recently-created SPs should appear normal (centered around zero) for a time, and then drop to anomalously low values. The opposite behavior may also occur, which would indicate that an SP has been healed. This preliminary analysis may be extended in the future to study creation and persistence of SPs over the entire history of ACS.

To find SPs that have been created since 2015, we begin with the SPs identified in the short dark from the 2016-10-19 anneal cycle. We then tabulate the depths of these same pixels in the short darks from all previous anneals after January 2015. Using a similar method to Anderson & Baggett (2014b), we step through each observation of the SP depths and calculate the mean depth from the preceding observations, and also the mean depth of the following observations. By removing these mean depths from the preceding and following observations, we can calculate a mean absolute residual for each observation. The optimal “break point” is the observation date for which the mean overall residual is minimized.

In Figure 9, we plot the pre- and post-break mean depths for each SP identified in the 2016-10-19 anneal cycle. The diagonal blue line corresponds to post-break values 2.5 times that of pre-break values, and the flat blue line corresponds to post-break values of  $-3 e^-$ . The  $\sim 7000$  pixels in the unshaded region have experienced particularly large jumps to negative depths. Inspection of the depths over time of several of these pixels confirms their recent creation. Assuming that these SPs turned on at a constant rate since January 2015, we find that  $\sim 290$  SPs are created per anneal cycle, which implies that around 53,000 SPs should have been created over the 14 year lifespan of ACS. Since we find about 65,000 SPs in recent

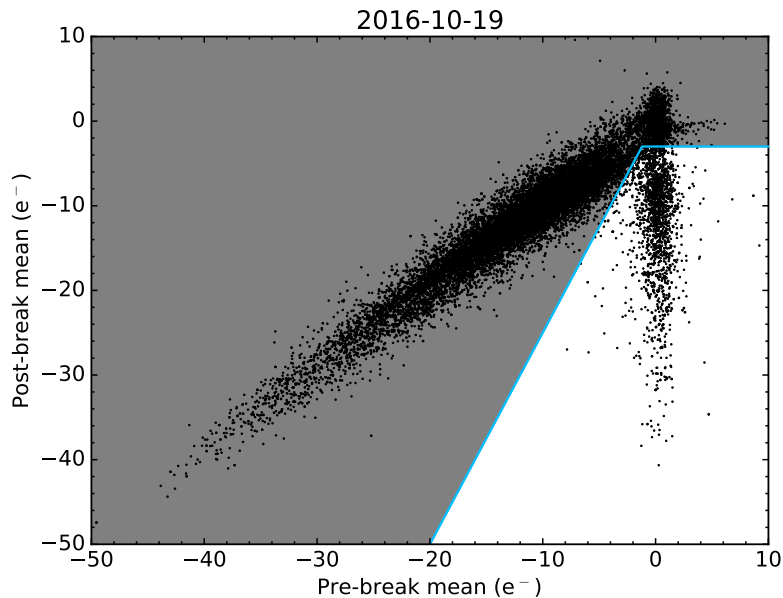


**Figure 9:** Pre- and post-break mean depths of 20,000 SPs randomly selected from the 2016-10-19 anneal. Mean depths were calculated by finding the observation date which minimized a mean overall residual for all of the observations. SPs that “turned on” recently lie in the cloud centered on a pre-break mean of zero. The blue lines and unshaded region represent our first attempt at selecting recently-created SPs.

anneals, this discrepancy suggests that perhaps the rate of SP creation is not constant, or that the detector had a distribution of sink pixels initially. The pixels in the diagonal cloud between  $(-40, -40)$  and  $(0, 0)$  have similar pre- and post-break means, suggesting that they have been consistently low for about two years, and therefore were likely created before 2015.

To find healed SPs, we perform the same analysis on SPs identified from the 2015-12-16 anneal cycle. We choose this anneal cycle because these pixels could potentially have returned to normal behavior afterwards, i.e., there’s no requirement for these pixels to be negative since 2015-12-16. We find 40 SPs with pre- and post-break means that suggest they could have “turned off” in 2016, but inspection of their depths over time show that only about 10 of them appear to return to normal behavior after displaying negative depths for many anneals. The remaining pixels have noisy or unstable behavior which prevents accurate selection of the break point. Therefore, healed SPs appear to be very rare, unless they can return to normal behavior gradually, which would be difficult to detect with our break-finding algorithm.

## 8 Conclusions & Next Steps

In this report, we have characterized sink pixels in ACS/WFC and have described a method for selecting and flagging them in images from 2015 onward. We identify SPs in the average short (0.5-second), flashed dark image from each monthly anneal cycle, and determine typical trail lengths for SPs of different depths and background levels. We create reference images that contain all of the information necessary to flag SPs, trailing low pixels, and high

downstream pixels, one for each anneal cycle since January 2015. These reference images will be used by CALACS to properly activate the charge trap flags in the DQ extensions of science images for SPs and the pixels they affect. We tested the application of these reference images on example data, and found that about 1 – 2% of the pixels in the detector were flagged, depending on the background level of the data. SPs appear to be created frequently, but rarely are they healed. A routine to generate reference images for future anneal cycles is being prepared for inclusion in the ACS/WFC reference file pipeline (Lim et al., 2012).

In the future, aspects of this study may be extended to the full history of ACS/WFC. An archive of all ACS/WFC images will soon be available, which will allow us to study the long-term behavior of SPs found in recent anneals. We can extend the analysis in Section 7 to determine the “turn on” dates of SPs created before 2015, and investigate more fully the rate of SP creation. Similarly, we can also determine the frequency with which SPs are healed.

## Acknowledgements

The authors would like to thank Russell Ryan and Sylvia Baggett for helpful discussions during this project. The authors would also like to thank the following ACS team members for their many useful comments: Jay Anderson, Roberto Avila, Andrea Bellini, David Borncamp, Marco Chiaberge, Samantha Hoffmann, Pey-Lian Lim, and Nathan Miles.

## References

- Anderson, J., & Baggett, S. 2014a, Sink Pixels and CTE in the WFC3/UVIS Detector, WFC3 ISR 2014-14, STScI
- . 2014b, Flagging the Sink Pixels in WFC3/UVIS, WFC3 ISR 2014-22, STScI
- Bohlin, R. C., Hartig, G., & Martel, A. 2001, HRC and WFC Flat Fields: Standard Filters, Polarizers, and Coronagraph, ACS ISR 2001-11, STScI
- Foreman-Mackey, D., Hogg, D. W., Lang, D., & Goodman, J. 2013, PASP, 125, 306
- Lim, P.-L., Ogaz, S., Armstrong, A., et al. 2012, Bias and Dark Calibration of ACS/WFC Data: Post-SM4 Automated Pipeline, ACS TIR 2012-01, STScI
- Ogaz, S., Anderson, J., & Golimowski, D. 2015, Post-Flash Calibration Darks for the Advanced Camera for Surveys Wide Field Channel (ACS/WFC), ACS ISR 2015-03, STScI